Photoreactions on $LaTiO_2N$ under Visible Light Irradiation

Asako Kasahara,[†] Kota Nukumizu,[†] Go Hitoki,[†] Tsuyoshi Takata,[†] Junko N. Kondo,[†] Michikazu Hara,[†] Hisayoshi Kobayashi,[‡] and Kazunari Domen*[,†,§]

Chemical Resources Laboratory, Tokyo Institute of Technology, Nagatsuta 4259, Midori-ku, Yokohama 226-8503, Japan, Kurashiki University of Science and the Arts, Nishinoura 2640, Tsurajima, Kurashiki 712-8505, Japan, and Core Research for Evolutional Science and Technology (CREST), Japan Society and Technology Co. (JST)

Received: April 17, 2002

Photochemical reactions on $LaTiO_2N$, a perovskite-type oxynitride, were examined. Under visible-light irradiation (420 nm < λ < 600 nm), $LaTiO_2N$ reduced H^+ into H_2 and oxidized H_2O into O_2 in the presence of a sacrificial electron donor (methanol) or acceptor (Ag^+) by the band gap transition (2.1 eV). Oxidation of water proceeded with little degradation of the oxynitride, whereas partial substitution of Ca^{2+} for La^{3+} of $LaTiO_2N$ and modification by IrO_2 colloid markedly suppressed degradation of the oxynitride and increased O_2 evolution efficiency.

Introduction

Various photocatalytic reactions have been studied for application to the removal of toxic organic and inorganic materials in air or solution. Much of this research has been focused on the use of TiO_2 powder; however, a range of new photocatalysts for overall water splitting, such as La-doped NiO/$NaTaO_3$ and $RuO_2/CaIn_2O_4$, have been reported.[1,2] All of these photocatalysts function under ultraviolet (UV) light irradiation (λ < 400 nm).[3−7] Photocatalysts that function in the visible region (400 nm < λ < 800 nm) are desirable from the viewpoint of solar energy utilization. Very recently, Asahi et al. have reported nitrogen-doped TiO_2 as a visible-light-driven photocatalyst for organic material degradation in air,[8] and Arakawa et al. found that photocatalytic overall water splitting proceeds over $InTaO_4$ under visible light irradiation.[9] In these photocatalysts, activation wavelengths are shorter than ca. 500 nm. The present authors have been investigating photocatalytic materials for the cleavage of water, including those activated by visible light such as $RbPb_2Nb_3O_{10}$, a Dion-Jacobson type layered perovskite. In the course of these studies, we found that some (oxy)nitrides and oxysulfides such as Ta_3N_5, TaON, $LaTiO_2N$, and $Sm_2Ti_2O_5S_2$ are stable materials which evolve H_2 or O_2 in the presence of appropriate sacrificial reagents. The common features of these materials based on our density functional theory (DFT) calculation of the electronic band structures are as follows: (1) The formal electronic configurations of transition metal cations are d^0. (2) The empty d orbitals form the bottoms of the conduction bands. (3) The tops of the valence bands consist primarily of N2p or S3p orbitals hybridized with O2p orbitals.

In this paper, we report photochemical reactions on $LaTiO_2N$, a typical oxynitride of titanium, in visible light. The schematic structure of $LaTiO_2N$ is illustrated in Figure 1. This brick-red∼dark brown oxynitride has the same structure as the perovskite oxide, represented ABO_3 (A, B: metal cations), and is composed of TiO_xN_y octahedral ($x + y = 6$).[10] Under visible light irradiation (420 nm < λ < 600 nm), $LaTiO_2N$ functioned for reduction of H^+ into H_2 and oxidation of H_2O into O_2 in the presence of the sacrificial electron donor (methanol) and acceptor (Ag^+), respectively.

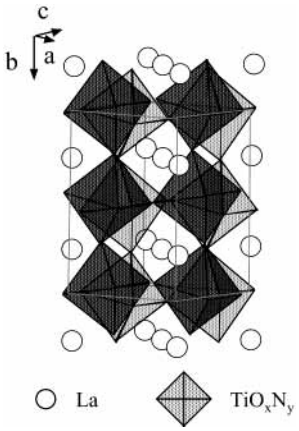

Figure 1. Schematic structure of $LaTiO_2N$.

Experimental Section

Preparation of Ti-Based Oxynitrides. $LaTiO_2N$ was prepared by heating an oxide precursor containing stoichiometric amounts of La^{3+} and Ti^{4+} (La:Ti = 1:1) cations under NH_3 flow. The metal-oxide precursor was prepared by the polymerized complex (PC) method.[11] A total of 5.7 g of titanium tetraisopropoxide and 8.7 g of $La(NO_3)_36H_2O$ were dissolved in 98.8 g of ethylene glycol at room temperature. 76.4 g of anhydrous citric acid, and 102.0 g of methanol was added to the solution, and the mixture was stirred at 403 K until a transparent gel was formed. The polymer was carbonized at 623 K and calcined in air at 923 K for 2 h to remove carbon. The precursor was nitrogenized by heating at 873−1223 K in an alumina tube under NH_3 flow (1 dm^3 min^{-1}). After 15 h, the sample was cooled to 773 K under NH_3 flow and then to room

* To whom correspondence should be addressed. E-mail: kdomen@res.titech.ac.jp.
† Tokyo Institute of Technology.
‡ Kurashiki University of Science and the Arts.
§ CREST.

10.1021/jp025961+ CCC: $22.00
Published on Web 06/28/2002

temperature under He flow to remove adsorbed NH_3. The powder obtained after heating for 15 h varied from orange to dark brown in color with increasing nitriding temperature.

$Ca_{0.25}La_{0.75}TiO_{2.25}N_{0.75}$, where Ca^{2+} is partially substituted for La^{3+} in $LaTiO_2N$, was also prepared by nitriding of a corresponding oxide precursor containing stoichiometric amounts of Ca^{2+}, La^{3+}, and Ti^{4+} (Ca:La:Ti = 0.25:0.75:1.00) cations in a similar manner as the preparation of $LaTiO_2N$ (15 h). The oxide precursor was synthesized from $CaCO_3$, titanium tetraisopropoxide and $La(NO_3)_36H_2O$ were synthesized by the PC method.

Modification by IrO_2 Colloid. IrO_2 colloid as an O_2 evolution catalyst was deposited onto the prepared oxynitrides. The colloid solution was prepared by hydrolysis of Na_2IrCl_6 in aqueous basic solution (pH12).[12,13] A total of 0.3 g of $LaTiO_2N$ or $Ca_{0.25}La_{0.75}TiO_{2.25}N_{0.75}$ sample and 10∼100 mL of the colloid solution (IrO_2: 0.5∼46.9 mg) were added to vigorously stirred distilled water (50 mL). After stirring for 30 min, a transparent supernatant solution was decanted, and the IrO_2-adsorbed sample was rinsed three times in distilled water. The sample was heated at 573 K under vacuum. The amounts of colloidal IrO_2 adsorbed onto the oxynitrides were estimated by measuring the 500−700 nm absorbance of the supernatant rinse solutions.

Photochemical Reactions. The reaction was carried out in a Pyrex reaction vessel connected to a closed gas circulation and evacuation system. Photoreduction of H^+ to H_2 and photooxidation of H_2O to O_2 in the presence of a sacrificial electron donor (methanol) and acceptor (Ag^+) were examined as test photoreactions. H_2 evolution was examined in an aqueous solution (200 mL) containing 0.20 g of the oxynitride loaded with 3 wt % Pt and 20 mL of methanol as a sacrificial electron donor. Pt was loaded by the impregnation method from $[Pt(NH_3)_4]Cl_2$, followed by reduction in H_2 at 573 K. In the case of typical photooxidation of water into O_2, the reaction performed in an aqueous $AgNO_3$ solution (0.01 mol dm^{-3}; 200 mL) containing 0.20 g of the oxynitride and 0.20 g of La_2O_3 powder. A basic oxide, La_2O_3, was added to maintain the pH of the solution at around 8 during the reaction (see below). The reaction solution was evacuated several times to remove air followed by irradiation with a 300 W−Xe lamp equipped with cutoff filters. The evolved gas was analyzed by gas chromatography.

Quantum efficiencies (Φ) were calculated using the following equation:

$$\Phi\ (\%) = (AR/\lambda) \times 100$$

where A, R, and I represent the coefficient based on the reactions (H_2 evolution, 1;[14] O_2 evolution, 4), the H_2 or O_2 evolution rate (molecules h^{-1}), and the rate of absorption of incident photons (9.6×10^{21} photons h^{-1} at 420 nm $< \lambda <$ 600 nm), respectively. The absorption rate of incident photons was measured by a Si photodiode. We assumed that the scattering of light was negligible and that visible light at $\lambda <$ 600 nm was available for the photoreactions because $LaTiO_2N$ and $Ca_{0.25}La_{0.75}TiO_{2.25}N_{0.75}$ did not work at $\lambda >$ 600 nm.

Results and Discussion

XRD Patterns, TEM Images and UV−vis Spectra of $LaTiO_2N$ and $Ca_{0.25}La_{0.75}TiO_{2.25}N_{0.75}$. Figure 2 shows X-ray diffraction (XRD) patterns of $LaTiO_2N$ and $Ca_{0.25}La_{0.75}TiO_{2.25}N_{0.75}$ prepared at 1223 K. The XRD pattern for $LaTiO_2N$ is consistent with that of perovskite-type $LaTiO_2N$.[10] The diffraction peaks were observed even for the sample nitrided at 973 K, and the intensity increased with nitriding temperature without the occurrence of impurity phases. Although there was no essential difference in XRD pattern between $LaTiO_2N$ and $Ca_{0.25}La_{0.75}TiO_{2.25}N_{0.75}$, each diffraction peak of $Ca_{0.25}La_{0.75}TiO_{2.25}N_{0.75}$ had slightly higher angles than that of $LaTiO_2N$. This indicates that in $Ca_{0.25}La_{0.75}TiO_{2.25}N_{0.75}$ Ca^{2+} cations are located in La^{3+} sites of the perovskite structure and that partial substitution of Ca^{2+} for La^{3+} reduces the lattice constant of $LaTiO_2N$ perovskite structures because Ca^{2+} (0.099 nm) has a smaller ionic radius than La^{3+} (0.106 nm). Elemental analysis (by differential thermal conductivity) revealed that N in $LaTiO_2N$ and $Ca_{0.25}La_{0.75}TiO_{2.25}N_{0.75}$ samples comprised about 70% of the stoichiometric amounts, suggesting that the prepared samples have a cation-defective perovskite structure, which may be similar to $La_{2/3\ 1/3}TiO_3$ (cation defect). In this paper, we refer to these samples as "$LaTiO_2N$" and "$Ca_{0.25}La_{0.75}TiO_{2.25}N_{0.75}$".

Transmission electron microscopy (TEM) images and UV−vis diffuse reflectance (DR) spectra of $LaTiO_2N$ prepared at 1223 K are shown in Figures 3 and 4, respectively. TEM

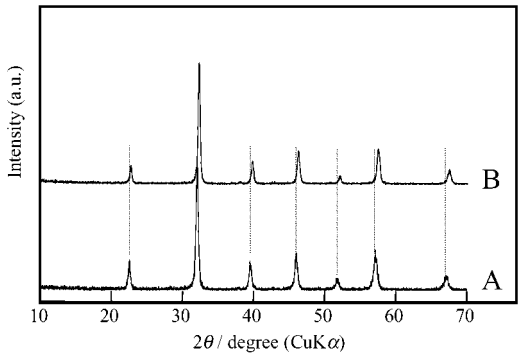

Figure 2. XRD pattern of $LaTiO_2N$ and $Ca_{0.25}La_{0.75}TiO_{2.25}N_{0.75}$ prepared at 1223 K. A: $LaTiO_2N$. B: $Ca_{0.25}La_{0.75}TiO_{2.25}N_{0.75}$.

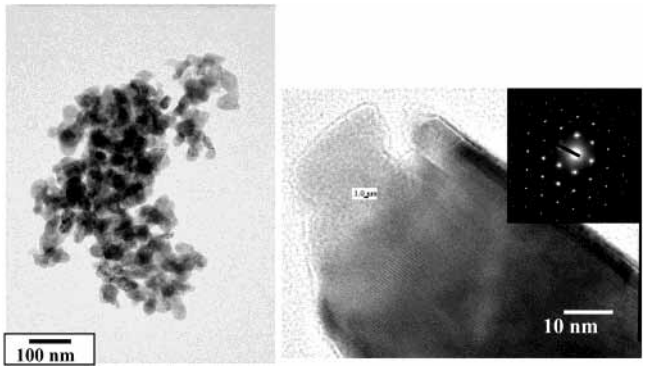

Figure 3. TEM images and electron diffraction pattern of $LaTiO_2N$ (1123 K).

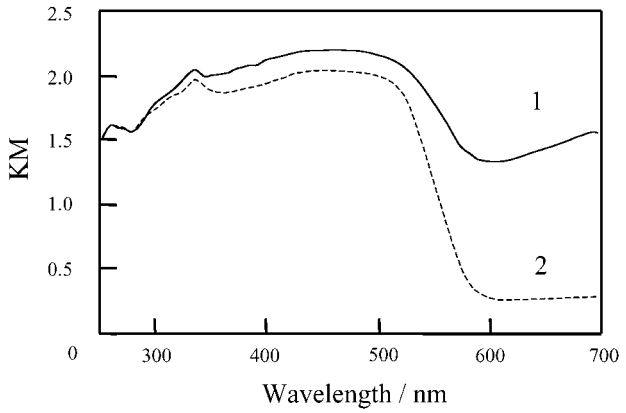

Figure 4. UV-vis DR spectra of $LaTiO_2N$. 1: Prepared $LaTiO_2N$. 2: After heating in air at 573 K for 24 h.

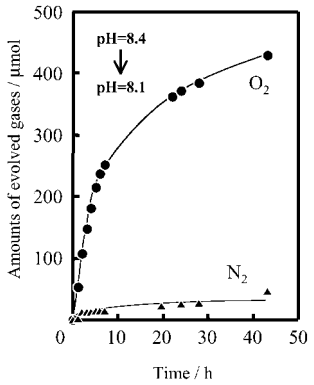

Figure 5. O_2 evolution from $LaTiO_2N$ under visible light irradiation (λ > 420 nm). $LaTiO_2N$: 0.2 g. La_2O_3: 0.2 g. 0.01 M $AgNO_3$ solution: 200 mL.

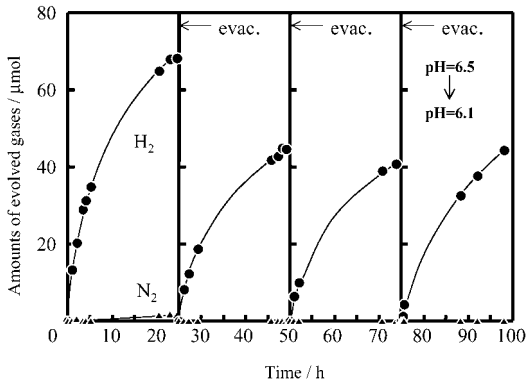

Figure 6. H_2 evolution from $LaTiO_2N$ under visible light irradiation (λ > 420 nm). Pt-deposited $LaTiO_2N$: 0.2 g, 200 mL methanol solution (distilled water, 160 mL; methanol, 40 mL).

observation revealed that primary particles of about 30∼70 nm in diameter aggregate to form large secondary particles of 0.5−20 μm. The TEM lattice image and electron diffraction pattern indicates that well-crystallized $LaTiO_2N$ is formed by nitriding for 15 h. The UV−vis spectrum consists of two broad bands. Heating the sample in air at 573 K for 24 h caused no change in the XRD pattern but weakened the band above 600 nm, indicating that the band in the near-infrared region is attributable to absorption due to a small amount of reduced Ti^{3+} species. Therefore, the charge-transfer band is extended to as long as ca. 600 nm, with a band gap energy of 2.1 eV. The TEM images and UV−vis DR spectrum for $Ca_{0.25}La_{0.75}TiO_{2.25}N_{0.75}$ were similar to those of $LaTiO_2N$, and the band gap energy was estimated to be ca. 2 eV.

Water Oxidation or Reduction by $LaTiO_2N$ under Visible Light Irradiation. Figure 5 shows a time course of O_2 evolution under visible light irradiation (λ > 420 nm). $LaTiO_2N$ prepared at 1223 K was used in the following photoreactions because the sample showed the highest activity for O_2 and H_2 evolution under visible light irradiation. The pH of the solution before and after the reaction are also shown in the figure. No reaction took place in the dark, and O_2 evolution began with the onset of irradiation. The rate of O_2 evolution decreased with reaction time as a result of the decrease in Ag^+ concentration, and the $LaTiO_2N$ surfaces became covered with reduced metallic Ag, turning the sample black. The initial quantum efficiency was ca. 1.5%, and the total O_2 evolved over 43 h is estimated to be 440 μmol. This amount corresponds to ca. 60% of the lattice oxygen in the catalyst (0.2 g of $LaTiO_2N$). There was no noticeable difference in the XRD pattern of the sample before and after the reaction, except for the emergence of a diffraction peak attributable to metallic Ag. The evolution of O_2 is therefore attributed to the oxidation of water on $LaTiO_2N$ under visible light irradiation. Figure 4 shows that a small amount of N_2 was coevolved with O_2 and is regarded as an oxidation product of $LaTiO_2N$, given by the reaction

$$2N^{3-} + 6h^+ \rightarrow N_2$$

From the total quantities of evolved O_2 and N_2 (O_2, 440 μmol; N_2, 40 μmol), it can be inferred that approximately 88% of photoexcited holes oxidize H_2O (or OH^-) into O_2 and the remaining 12% of holes oxidize N^{3-} (in $LaTiO_2N$) into N_2. This indicates that $LaTiO_2N$ is partially degraded under the photoreaction condition. Interestingly, at pH below 7, O_2 evolution was suppressed while N_2 evolution proceeded, indicating that the efficient oxidation of water requires a relatively high concentration of OH^-. It is therefore concluded that in alkaline solutions $LaTiO_2N$ oxidizes water to O_2 with a little degradation of itself.

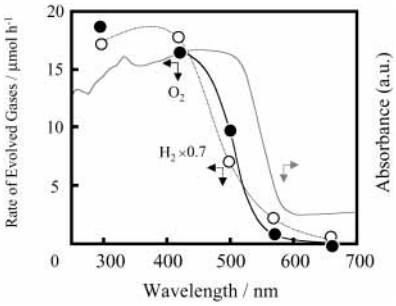

Figure 7. Dependence of the initial rates of H_2 and O_2 on cutoff wavelength of incident light and UV−vis DR spectrum of $LaTiO_2N$. H_2: Pt-deposited $LaTiO_2N$ (0.2 g), 200 mL methanol solution (distilled water, 160 mL; methanol, 40 mL). O_2: $LaTiO_2N$ (0.2 g). La_2O_3: 0.2 g, 200 mL 0.01 mol dm^{-3} $AgNO_3$ solution. UV−vis DR spectrum: $LaTiO_2N$ after heating in air at 573 K for 24 h.

Figure 6 shows the evolution of H_2 from an aqueous methanol solution. Again, without irradiation, no reaction took place. The initial quantum efficiency for H_2 evolution in the first reaction was estimated to be about 0.15%. The rate of H_2 evolution in the second and subsequent runs with intermittent evacuation was somewhat slower than that of the first run but continued to proceed steadily. Up to 1.6 μmol of N_2 was detected in the first run but was not detectable by gas chromatography after the second run. Therefore, it is concluded that the oxynitride was stable during the reaction.

The relationship between the H_2 and O_2 evolution rates and the cutoff wavelength of incident light is shown in Figure 7. The initial rate of H_2 and O_2 evolution decreases with increasing cutoff wavelength, and the longest wavelength available for either photoreaction was estimated to be ca. 600 nm, corresponding to the absorption edge for $LaTiO_2N$. These photoreactions proceed via the band gap transition.

Oxidation of Water by IrO_2-Adsorbed $Ca_{0.25}La_{0.75}TiO_{2.25}N_{0.75}$. It is worth noting that when we partially substituted Ca^{2+} for La^{3+} and modified the material using IrO_2 colloid (i.e., $IrO_2/Ca_{0.25}La_{0.75}TiO_{2.25}N_{0.75}$), the O_2 evolution rate increased with suppression of degradation of the material. To improve activity for oxidation of water and prevent degradation during water oxidation, the absorption of IrO_2 colloid on the oxynitrides was examined. Although the IrO_2 colloid was not adsorbed by $LaTiO_2N$, $Ca_{0.25}La_{0.75}TiO_{2.25}N_{0.75}$ absorbed considerable amounts of IrO_2 colloid as an O_2 evolution catalyst. The maximum amount of loaded IrO_2 colloid was estimated to be 11 wt %.

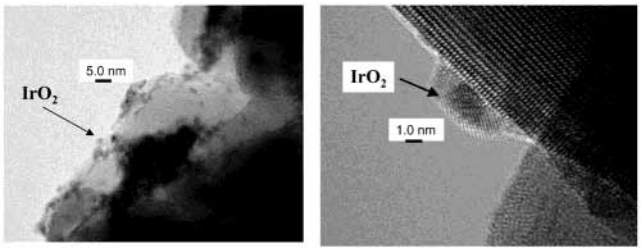

Figure 8. TEM images of 2 wt % $IrO_2/Ca_{0.25}La_{0.75}TiO_{2.25}N_{0.75}$ (1223 K).

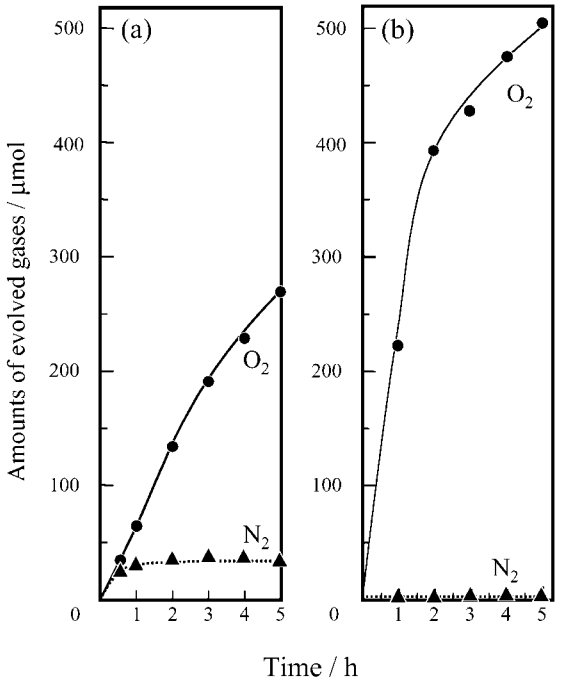

Figure 9. O_2 evolution from $Ca_{0.25}La_{0.75}TiO_{2.25}N_{0.75}$ and 2 wt % $IrO_2/Ca_{0.25}La_{0.75}TiO_{2.25}N_{0.75}$ under visible light irradiation ($\lambda > 420$ nm). (a) $Ca_{0.25}La_{0.75}TiO_{2.25}N_{0.75}$. (b) 2 wt % $IrO_2/Ca_{0.25}La_{0.75}TiO_{2.25}N_{0.75}$. $Ca_{0.25}La_{0.75}TiO_{2.25}N_{0.75}$, 2 wt % $IrO_2/Ca_{0.25}La_{0.75}TiO_{2.25}N_{0.75}LaTiO_2N$: 0.2 g. La_2O_3: 0.2 g. 0.01 M $AgNO_3$ solution: 200 mL.

Figure 8 shows TEM images of $Ca_{0.25}La_{0.75}TiO_{2.25}N_{0.75}$ loaded with 2 wt % IrO_2 colloid (2 wt % $IrO_2/Ca_{0.25}La_{0.75}TiO_{2.25}N_{0.75}$). IrO_2 colloid particles of several nanometers in diameter are deposited on $Ca_{0.25}La_{0.75}TiO_{2.25}N_{0.75}$ surfaces. Figure 9 shows time courses of O_2 evolution on $Ca_{0.25}La_{0.75}TiO_{2.25}N_{0.75}$ and 2 wt % $IrO_2/Ca_{0.25}La_{0.75}TiO_{2.25}N_{0.75}$ under visible light irradiation ($\lambda > 420$ nm). $Ca_{0.25}La_{0.75}TiO_{2.25}N_{0.75}$ was prepared at 1223 K. There was no noticeable difference in O_2 evolution between $LaTiO_2N$ and $Ca_{0.25}La_{0.75}TiO_{2.25}N_{0.75}$. However, $IrO_2/Ca_{0.25}La_{0.75}TiO_{2.25}N_{0.75}$ showed a higher activity for O_2 evolution than $LaTiO_2N$ and $Ca_{0.25}La_{0.75}TiO_{2.25}N_{0.75}$, and the initial quantum efficiency reached ca. 5%. Furthermore, N_2 evolution was markedly suppressed using this alternative material. With the evolution of 500 μmol of O_2 (5 h irradiation), only 4 μmol of N_2 was produced; that is, 99% of the holes were used for water oxidation. This result clearly demonstrates that with the appropriate modification of $LaTiO_2N$ or and $Ca_{0.25}La_{0.75}TiO_{2.25}N_{0.75}$ it is possible to stabilize this system by kinetic control with respect to degradation of the oxynitride. In $IrO_2/Ca_{0.25}La_{0.75}TiO_{2.25}N_{0.75}$, the rate of O_2 evolution increased with increasing loaded IrO_2 colloid, reaching a maximum at 2 wt %. Further adsorption of IrO_2 colloid beyond 2 wt % decreased O_2 evolution rate.

To summarize the results, $LaTiO_2N$ under visible light irradiation oxidizes water into O_2 or reduces H^+ into H_2 in the presence of appropriate sacrificial reagents by the band gap transition. This indicates that $LaTiO_2N$ is a visible-light driven material with sufficient reduction and oxidation potentials. Although a part of $LaTiO_2N$ is degraded during photooxidation of water, it is possible to suppress this degradation by appropriately modifying the catalytic system.

As yet we have not successfully achieved overall water splitting using $LaTiO_2N$-based material. Compared with the efficiency of O_2 evolution, the H_2 evolution efficiency, ca. 0.15%, is still low. This appears to be due to poor dispersion of loaded Pt, resulting in low efficiency of electron transfer to H^+. Appropriate surface modification by H_2 evolution catalyst might improve H_2 evolution efficiency. This possibility is currently under investigation.

Acknowledgment. This work was supported by the Core Research for Evolutional Science and Technology (CREST) program of the Japan Science and Technology Co. (JST).

References and Notes

(1) Kato, H.; Kudo *J. Phys. Chem. B* **2001**, *105*, 4285.
(2) Sato, N.; Nishiyama, H.; Inoue, Y. *J. Phys. Chem. B* **2001**, *105*, 6061.
(3) Schiavello, M. *Heterogeneous Photocatalysis*; John Wiley & Sons: London, 1997.
(4) Domen, K.; Naito, S.; Onishi, T.; Tamaru, K.; Soma, M. *J. Phys. Chem.* **1982**, *86*, 3657.
(5) Kudo, A.; Domen, K.; Tanaka, A.; Maruya, K.; Aika, K.; Onishi, T. *J. Catal.* **1988**, *111*, 67. Takata, T.; Furumi, Y.; Shinohara, K.; Tanaka, A.; Hara, M.; Nomura, J. K.; Domen, K. *Chem. Mater.* **1997**, *9*, 1063.
(6) Sayama, K.; Arakawa, H. *J. Phys. Chem.* **1993**, *97*, 531.
(7) Kudo, A.; Kato, H.; Nakagawa, S. *J. Phys. Chem. B* **2000**, *104*, 571.
(8) Asahi, R.; Morikawa, T.; Ohwaki, T.; Aoki, K.; Taga, Y. *Science* **2001**, *293*, 269.
(9) Zou, Z.; Ye, J.; Sayama, K.; Arakawa, H. *Nature* **2001**, *414*, 625.
(10) Gendre, L. L.; Marchand, R.; Piriou, B. *Eur. J. Solid State Inorg. Chem.* **1997**, *34*, 973.
(11) Kakihana, M. *J. Sol-Gel Sci.* **1996**, *5*, 7.
(12) Harriman, A.; Thomas, J. M.; Millward, G. R. *New J. Chem.* **1987**, *11*, 757.
(13) Harriman, A.; Pickering, I. J.; Thomas, J. M.; Christensen, P. A. *J. Chem. Soc., Faraday Trans. 1* **1988**, *84*, 2795.
(14) In the case of methanol, we assume that one photon forms a H_2 molecule because of current doubling effect.